Identification of novel pyrazole and pyrazolone derivatives with anti-cancer, antioxidant and anti-tyrosinase properties: Synthesis, *In-vitro* biological and computational evaluation.

Samuel T. Boateng, Tithi Roy, Sergette Banang-Mbeumi, Siva Murru and Jean Christopher Chamcheu
University of Louisiana at Monroe, LA

INTRODUCTION

- **The promising and dynamic pharmacological effects of heterocyclic five-membered aromatic ring family; pyrazole and pyrazolone have encourage their utilization as chemo-type in drug design. Many of their resulting therapeutic agents have been shown to be potent, safe, cheaper and efficacious in the management of cancer, infections, inflammations and other chronic diseases.**
- **Among the 78 organs of the human body, the skin is the largest and visible of them all; which serves as a shield against mechanical, thermal, microbial and physical insult. This makes skin conditions a complete deviant to health; where the presence of the disease significantly impaired physical, mental and social well-being. Skin cancer (SC) and pigmentation disorders falls are culprit to these perilous discomfort patients are subjected to. Despite the advancement being made in their management, these both chronic conditions, are showing less vulnerable to existing therapy due to side-effects, drug resistance, low-bioavailability etc.**
- **In this project, 25 compounds of the pyrazole and pyrazolone family were synthesized and tested for their anticancer, tyrosinase inhibitory(which is mostly elevated in pigmentation disorders disorders) and antioxidant affect. This is envisioned to identify promising agents which may update and help assuage some of the challenges associated with SC and pigmentation disorder management.**

OBJECTIVES

To synthesize and evaluate the anti-tyrosinase, anticancer and antioxidant activity of pyrazole and pyrazolone compounds.

METHODS

Chemical Synthesis: The microwave assisted synthesis of pyrazoles and pyrazolones from unsymmetrical dicarbonyl derivatives and base-metal catalyzed regioselective synthesis approach.

Cell culture: The human NMSC cells (A431 and SCC-12), MSC cells (A375 and SKM-el-28) and nontumorigenic immortalized keratinocytes cells (HaCaT) were cultured in DMEM medium supplemented with 5-10% fetal bovine serum and 1% antibiotic penicillin. The cells were maintained under standard cell culture conditions at 37° C and 5% CO_2 in a humid environment.

DPPH free radical scavenger assay: The antioxidant potential of the synthesized derivatives was determined based on their ability to scavenge the 2,2'-diphenyl-1-picyrlhydrazl (DPPH) radical and the assays were conducted in a 96-well format.

In-vitro mushroom tyrosinase inhibition assay: Mushroom tyrosinase, L-tyrosine and positive control, arbutin and kojic acid were used in tyrosinase inhibition assays performed in a 96-well microplate format using a SpectraMax M2 microplate reader, operated by SoftmaxPro v.4.6 software (Molecular Devices, CA, USA).

Cell viability assay: The cell viability of cells were determined by the 3-(4,5-dimethylthiazol-2-yl)-2,5-diphenyltetrazolium bromide (MTT) assay after a 96-well plate seeded with cells were treated at 60-70% confluence and analyzed after 48hrs using Synergy multi-mode reader at 570nm.

In vitro wound healing assay: Artificial scratch wounds were inflicted on confluent monolayer cells using a Gilson pipette tip and were treated with/without test compound. Light microscopic images (20x) of the wounds were captured immediately after adding test compound (0 h) and after 48 h of treatment. The distances between the edges of the wounds were measured and average values determined as an indicator of wound closure over 48 h.

Colony Formation assay/Western Blotting: A previously treated 10cm plate of about 3000 cells for 48 h were plated in drug free medium and incubated for 10 days until control cells reached about 90% confluency or cell plates formed about 50-150 colonies. The plates were then harvested and fixed 5% gentian violet staining agent in 64% (v/v) methanol and 4% paraformaldehyde (4% PFA) then washed, dried, photographed and analyzed using counted and analyzed using the count and Plot Histograms of Colony Size (countPHICS) analysis tool. Protein lysates were electrophoresed and incubated with appropriate antisera. Blots were exposed to ECL and autoradiographed on a BioRad imaging system. Equal protein loading was ensured by stripped and reprobed membranes with appropriate controls. Densitometric analyses of the visualized protein bands were performed using BioRad Quantity One.**Virtual ADME/TOX screening**: The SwissADME web-tool was used to assessed the pharmacokinetic and pharmacodynamics properties of the active hits.

Molecular Docking: It was done using SwissTargetPrediction web-based tool and analyzed using the BIOVIA DiscoveryStudio software.

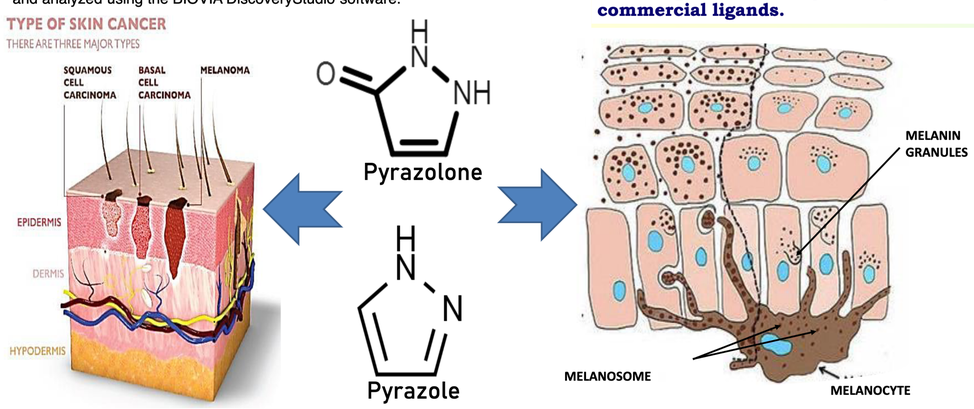

Figure 1: A scheme showing the scaffold of the pyrazole and pyrazolone as potential agent against skin cancer and pigmentation disorders.

RESULTS

Cell lines- IC_{50} values in µM (selectivity index)					
CPD ID	MELANOMA		NON-MELANOMA		CONTROL
	A375	SKMEL-28	GFP-A431	SCC-12	HaCaT
P1	47.7±4.2	42.8±0.3	41.6±0.8	257.3±18.4	60.5±3.9
P2	54.3±1.6	42.6±1.5	43.9±2.1	245.6±37.3	44.2±1.1
P3	54.8±2.7	59.1±4.6	27.2±0.9 (1.6)	546.5±20.7 (0.1)	42.1±3.4
P4	58.4±4.5	62.3±2.7	70.8±6.2	215.8±13.4	76.1±0.0
P5	65.3±4.2	130.9±2.4	42.1±3.1(6.3)	77.6±1.7(3.4)	265.4±4.3
P6	113.5±3.3	47.4±1.2	69.8±7.5(2.1)	49.9±3.4 (3.0)	147.2±0.8
P7	53.3±4.2	46.0±1.0	47.8±2.0	43.0±2.1	59.2±3.5
P8	55.3±3.8	180.9±4.7	72.2±5.2	120.0±8.5	44.5±1.4
P9	45.2±2.0	40.8±1.0	28.0±3.6 (1.6)	28.8±1.4 (1.5)	43.6±1.4
P10	55.3±2.5	43.7±2.7	195.5±3.8	49.1±2.0	68.0±1.2
P11	57.8±6.5	34.5±1.2	43.7±2.7 (2.6)	44.6±1.3(2.6)	115.5±10.1
P12	73.5±3.8	24.0±2.0	55.5±3.5	32.6±2.1	32.6±2.4
P13	93.4±6.4	153.5±2.9	181.4±4.7	52.8±2.2	91.6±4.1
P14	25.8±2.7	33.3±1.7	17.8±0.5 (2.0)	42.5±2.8 (0.8)	35.1±2.8
P15	58.5±3.4	36.0±3.9	42.9±1.0	98.0±5.5	53.7±3.1
P16	46.0±1.0	39.1±2.3	21.0±1.3 (2.6)	19.6±2.0 (2.8)	54.2±3.6
P17	44.5±3.0	34.2±3.9	19.7±0.8 (3.7)	23.4±1.7 (3.1)	72.4±6.0
P18	48.0±2.1	19.3±2.4	25.9±0.9 (2.0)	21.9±0.2 (2.3)	49.6±1.5
P19	47.1±4.2	40.5±3.0	7.6±0.6 (7.5)	97.9±5.6 (0.6)	57.0±1.3
P20	109.8±15.4	50.0±4.3	119.6±2.6	57.3±0.2	47.7±2.7
P21	67.8±2.3	42.7±4.0	58.6±2.3	37.8±3.2	50.1±6.5
P22	28.7±1.2	31.3±2.4	12.6±1.6 (3.8)	18.7±1.4 (2.6)	47.6±1.6
P23	31.2±1.5	27.4±2.3	23.9±1.0 (1.7)	21.7±1.9 (1.9)	40.5±1.5
P24	56.4±1.7	54.1±1.9	18.6±0.9 (3.3)	140.8±3.9 (0.4)	60.4±3.2
P25	**14.3±0.9**	**7.6±0.6**	**3.7±0.5 (8.2)**	**12.2±0.6 (2.5)**	**30.5±2.0**
[c]Cisplatin	1.49±0.44	14.2±0.24	7.7±0.3 (0.4)	4.4±0.2 (0.8)	3.4±0.4

Table 1: Cytotoxicity P1-P25 against human cutaneous melanoma (A375 & SK-Mel-28) and non-melanoma skin cancer (A431 & SCC12) cells relative to standard control HaCaT cells.

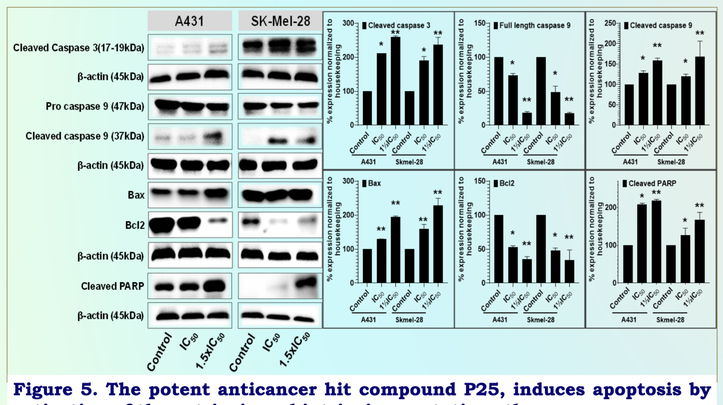

Figure 5. The potent anticancer hit compound P25, induces apoptosis by activating of the extrinsic and intrinsic apoptotic pathway caspases

Ligands	Kinase				Oxidoreductase		Other targets				
	MAPK 14/p38α	VEGFR1	Tyrosine protein kinase FLT3	JAK1	COX-1	COX-2	Alpha-2b AR	Carbonic anhydrase II	HSP 90-alpha	Cytochrome P450	Tyrosinase
Natural	-13.4	-10.7	-7.7	-6.4	-10.6	10.3	-8.5	-10.4	-7.2	-9.6	- 5.90
Clinical Ligand	PH-797804 -8.2	Sorafenib -10.7	Gilteritinib -7.7	Tofacitinib -8.6	Celecoxib -10.0	Celecoxib -11.0	Imiloxan -7.8	Dorzolamide -7.2	Geldanamycin -7.6	Clarithromycin -10.2	Kojic acid --5.80
3	-7.6	-7.5	-7.1	-6.6	-6.8	-7.2	-7.3	-6.4	-6.2	-7.4	-6.10
4	-8.1	-7.5	-7.2	-6.6	-7.1	-7.1	-7.8	-6.3	-6.3	-7.8	-6.50
6	-9.1	-8.0	-8.6	-8.2	-7.9	-8.7	-8.2	-7.1	-6.9	-8.7	-7.00
8	-9.1	-7.9	-8.5	-7.6	-7.8	-8.0	-8.5	-7.2	-7.1	-8.5	-6.70
9	-10.3	-8.8	-8.7	-9.1	-10.2	-10.1	-8.5	-9.3	-8.2	-9.9	-6.70
11	-7.7	-7.5	-7.2	-6.6	-6.8	-7.2	-7.4	-6.4	-6.1	-7.4	-6.10
12	-9.2	-7.5	-8.9	-7.8	-7.8	-8.7	-8.1	-7.4	-7.6	-8.3	-7.20
14	-9.5	-6.3	-8.9	-8.3	-8.8	-8.5	-7.9	-7.9	-7.2	-8.4	-6.00
17	-9.1	-6.7	-9.2	-8.5	-9.6	-9.2	-8.1	-8.0	-7.4	-8.1	-6.40
18	-9.8	-7.0	-8.9	-8.4	-9.6	-9.0	-7.9	-8.1	-7.5	-8.0	-6.70
19	-9.0	-7.5	-8.5	-9.1	-9.1	-10.5	-6.4	-8.2	-7.2	-8.9	-6.40
21	-9.2	-9.3	-8.6	-7.7	-8.9	-9.3	-7.2	-8.5	-7.6	-8.5	-6.70
22	-7.6	-10.2	-8.9	-8.3	-7.8	-8.6	-4.1	-7.5	-6.9	-8.0	-5.80
23	-8.3	-11.3	-10.3	-9.2	-8.2	-9.3	-4.1	-8.3	-7.7	-9.5	-6.50
24	-8.6	-9.7	-8.8	-8.0	-9.0	-8.9	-5.9	-7.9	-7.4	-8.6	-6.20
25	-8.5	-9.8	-8.7	-8.0	-8.8	-9.0	-4.8	-7.7	-7.8	-8.9	-6.40

Table 2: Binding affinity of the promising hit compounds toward molecular targets including kinases, enzymes, lyase, and oxidoreductase compared to their natural and commercial ligands.

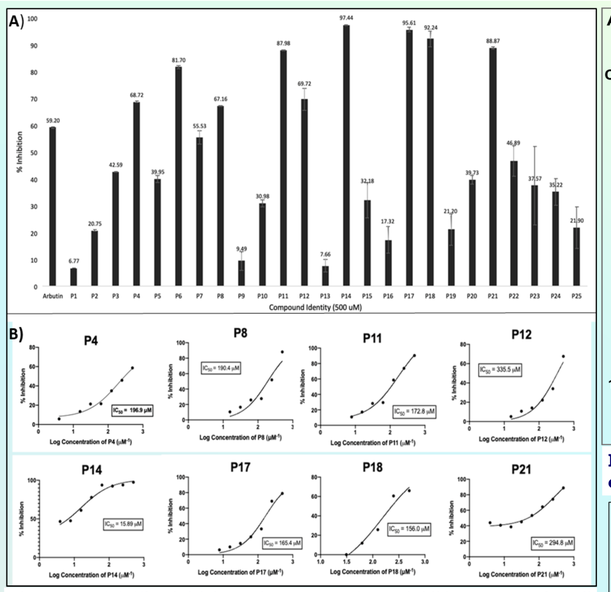

Figure 2: (A) The initial mushroom tyrosinase inhibitory assay for all compounds, with Arbutin as a positive control. (B) The dose-response curve of the potent compounds. Data are expressed as the mean ± SD from at least six independent experiments performed in quadruplicates.

Figure 3: Docking interaction between P4, P8, P11, P12, P14, P17, P18, P21, P25 and Kojic Acid, and the target tyrosinase protein. The target protein is highlighted in line ribbon format with light grey color. The active binding site amino acids are highlighted in black color. A) line and stick representation. B) Ball and stick model illustration.

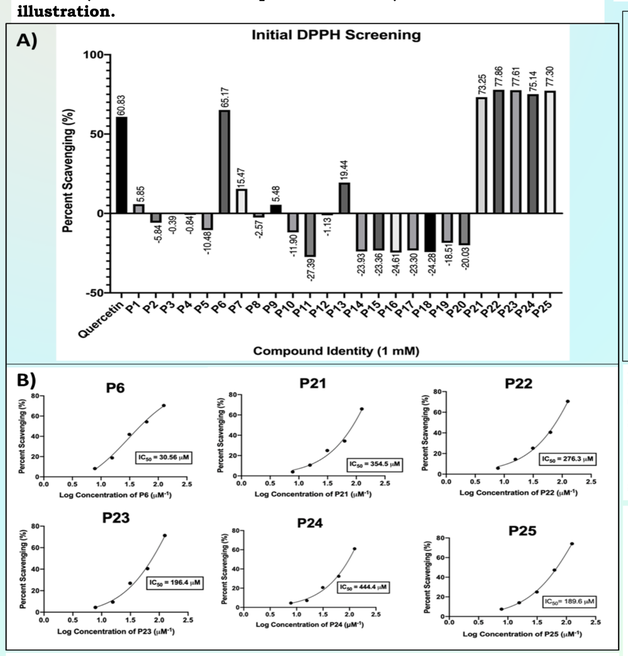

Figure 4: The 2,2-diphenyl-1-picrylhydrazyl (DPPH) anti-oxidant activities of all compounds using Quercetin as a positive control.

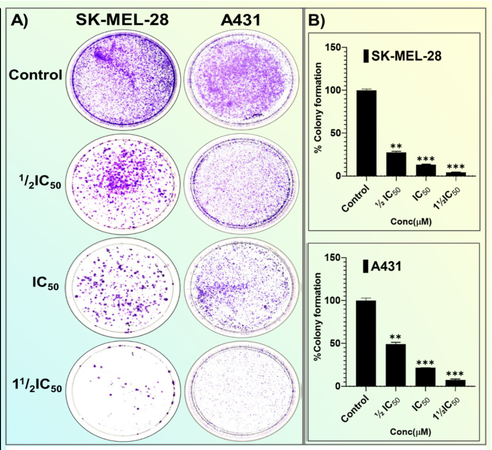

Figure 6: The potent P25, significantly inhibits colony formation capacity.

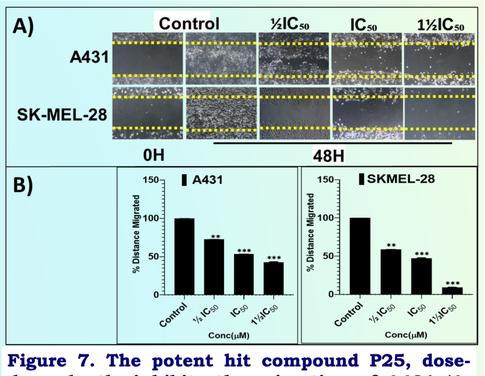

Figure 7. The potent hit compound P25, dose-dependently inhibits the migration of A431 (A; top panel) and SK-MEL-28 (A; bottom panel) cells in-vitro into the cell-free wounded scratched areas of a confluent cell monolayer.

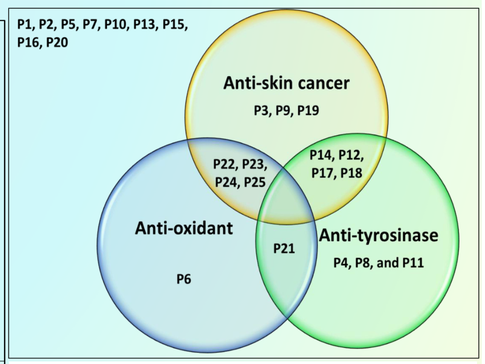

Figure 8: The Venn diagram provides a summary of the anti-proliferative (anti-skin cancer), antioxidant and tyrosinase inhibitory effect of the all 25 compounds which identifies 16 promising hits with either single or dual activity.

ACKNOWLEDGEMENTS

Support from the following sources is gratefully acknowledged:

- **NIH NIGMS P20GM12345 grant (Institutional Development Award (IDeA))**
- **Board of Regent of Louisiana RCS grant LEQSF(2021-24)-RD-A-22**
- **SD 2022 Travel Award**
- **SID 2022 Future leader retreat Award**

To find our lab SCAN HERE!

CONCLUSION & FUTURE PERSPECTIVES

- **In this study, novel compounds were synthesized and identified for their inherent anti-skin cancer, anti-tyrosinase and anti-oxidant activity.**
- **The most potent anti-cancer (P25) and anti-tyrosinase (P14) in the future, could be modified to amplified its observed pharmacological activity for further investigation in-vivo.**
- **The molecular mechanism accounting for the observed effects of these potent compounds could be probe using RNA-seq.**

REFERENCES

•Trager MH et al. (2020), Advances in Prevention and Surveillance of Cutaneous Malignancies. Am J Med. 133(4):417-423. doi: 10.1016/j.amjmed.10.008.

•Daina, A. et al.(2019). SwissTargetPrediction: updated data and new features for efficient prediction of protein targets of small molecules. Nucleic acids research, 47(W1), W357-W364.